

Substitution Chemistry of Gallium for Titanium in Nonlinear Optical KTiOPO_4 : Syntheses and Single-Crystal Structures of $\text{KGaF}_{1-\delta}(\text{OH})_\delta\text{PO}_4$ ($\delta \approx 0.3$) and $\text{KGa}_{0.5}\text{Ge}_{0.5}(\text{F},\text{OH})_{0.5}\text{O}_{0.5}\text{PO}_4$

William T. A. Harrison*,†

Department of Chemistry, University of Houston, Houston, Texas 77204-5641

Mark L. F. Phillips

Department 1846, Sandia National Laboratories, Albuquerque, New Mexico 87185-0333

Galen D. Stucky

Department of Chemistry, University of California, Santa Barbara, California 93106-9510

Received February 28, 1995. Revised Manuscript Received August 1, 1995*

The syntheses, single-crystal structures, and optical properties of $\text{KGaF}_{1-\delta}(\text{OH})_\delta\text{PO}_4$ ($\delta \approx 0.3$) and $\text{KGa}_{0.5}\text{Ge}_{0.5}(\text{F},\text{OH})_{0.5}\text{O}_{0.5}\text{PO}_4$, two structural analogues of potassium titanyl phosphate, KTiOPO_4 (KTP), are described. Both phases crystallize in the typical noncentrosymmetric $Pna2_1$ space group adopted by KTP-type materials, but the powder second harmonic generation responses of $\text{KGaF}_{1-\delta}(\text{OH})_\delta\text{PO}_4$ and $\text{KGa}_{0.5}\text{Ge}_{0.5}(\text{F},\text{OH})_{0.5}\text{O}_{0.5}\text{PO}_4$ are negligible compared to that of KTiOPO_4 . $\text{KGaF}_{1-\delta}(\text{OH})_\delta\text{PO}_4$ shows exclusive preferential substitution of fluoride ions into the octahedral-chain oxygen atom sites, and the resulting $\text{GaO}_4\text{F}_{2-\delta}(\text{OH})_\delta$ octahedra do not show the typical octahedral distortion found in Ti-containing KTP phases. $\text{KGa}_{0.5}\text{Ge}_{0.5}(\text{F},\text{OH})_{0.5}\text{O}_{0.5}\text{PO}_4$ shows no detectable Ga/Ge cation ordering, but an unusual, partial disordering of both the extraframework potassium cations occurs. Members of the $\text{KGa}_x\text{Ti}_{1-x}(\text{F},\text{OH})_x\text{O}_{1-x}\text{PO}_4$ solid solution series have been prepared as powders, and various trends across this series are reported. Crystal data: $\text{KGaF}_{1-\delta}(\text{OH})_\delta\text{PO}_4$: $M_r = \sim 222.79$, orthorhombic, space group $Pna2_1$ (No. 33), $a = 12.717(2)$ Å, $b = 6.3021(8)$ Å, $c = 10.431(2)$ Å, $V = 836(2)$ Å³, $Z = 8$, $R(F) = 3.32\%$ for 1479 observed reflections with $I > 3\sigma(I)$. $\text{KGa}_{0.5}\text{Ge}_{0.5}(\text{F},\text{OH})_{0.5}\text{O}_{0.5}\text{PO}_4$: $M_r = 222.73$, orthorhombic, space group $Pna2_1$ (No. 33), $a = 12.756(2)$ Å, $b = 6.306(1)$ Å, $c = 10.413(2)$ Å, $V = 838(2)$ Å³, $Z = 8$, $R(F) = 3.35\%$ for 1332 observed reflections [$I > 3\sigma(I)$].

Introduction

Potassium titanium phosphate, KTiOPO_4 (KTP), is of great current interest due to its exceptional electrooptic and physical properties,^{1,2} especially in the second harmonic generation (SHG) of 1064 nm Nd:YAG laser radiation.³ Over the past few years, it has become apparent that the KTP-type structure is extremely accommodating with respect to partial or complete isomorphous substitution,^{4–10} which may be especially

significant in optical device applications such as waveguides.^{11,12}

The study of KTP-type isomorphous-substitution compounds gives valuable insight into the mechanism of SHG at the atomic level^{2,10} in this class of materials. Like all SHG-active crystals, the KTiOPO_4 structure is noncentrosymmetric,¹³ and its most important microstructural feature in terms of optical behavior is believed to be the infinite, helical, vertex-sharing chains of distorted octahedral TiO_6 groups, cross-linked by phosphorus atoms (as PO_4 groups) into an open, three-dimensional structure.^{2,10} The two crystallographically distinct TiO_6 octahedra in KTiOPO_4 are both highly distorted, and a chain of short ($d < 1.75$ Å) and long ($d > 2.10$ Å) Ti–O bonds propagates through the crystal, in alternating –short–long–short–long– form. Substitution of vanadium(IV) for titanium, resulting in $\text{KTi}_{1-x}\text{V}_x\text{OPO}_4$,¹⁴ has little effect on the magnitude of SHG response, except for absorption effects. However,

† Present address: Department of Chemistry, University of Western Australia, Nedlands, WA 6907, Australia.

* Abstract published in *Advance ACS Abstracts*, September 1, 1995.

(1) Zumsteg, F. C.; Bierlein, J. D.; Gier, T. E. *J. Appl. Phys.* **1976**, *47*, 4980.

(2) Stucky, G. D.; Phillips, M. L. F.; Gier, T. E. *Chem. Mater.* **1989**, *1*, 492.

(3) Bierlein, J. D.; Vanherzeele, J. *J. Opt. Soc. Am.* **1989**, *B6*, 622.

(4) Phillips, M. L. F.; Harrison, W. T. A.; Stucky, G. D. *Inorg. Chem.* **1990**, *29*, 3245.

(5) El Haidouri, A.; Durand, J.; Cot, L. *Mater. Res. Bull.* **1990**, *25*, 1193.

(6) Crosnier, M.-P.; Guyomard, D.; Verbaere, A.; Piffard, Y. *Eur. J. Solid State Inorg. Chem.* **1990**, *27*, 845.

(7) Crennell, S. J.; Owen, J. J.; Grey, C. P.; Cheetham, A. K.; Kaduk, J. A.; Jarman, R. H. *J. Mater. Chem.* **1991**, *1*, 113.

(8) Phillips, M. L. F.; Gier, T. E.; Eddy, M. M.; Keder, N. L.; Stucky, G. D.; Bierlein, J. D. *Solid State Ion.* **1989**, 147.

(9) Phillips, M. L. F.; Anderson, M. T.; Sinclair, M. B. In *Proc. Lasers '93*; Corcoran, V. I., Goldman, T. S., Eds.; STS Press: McLean, VA, 1994; pp 733–740.

(10) Phillips, M. L. F.; Harrison, W. T. A.; Stucky, G. D.; McCarron, III, E. M.; Calabrese, J. C.; Gier, T. E. *Chem. Mater.* **1992**, *4*, 222.

(11) Risk, W. P. *Appl. Phys. Lett.* **1991**, *58*, 19.

(12) Thomas, P. A.; Glazer, A. M. *J. Appl. Cryst.* **1991**, *24*, 968.

(13) Tordjman, I.; Masse, R.; Guitel, J. C. *Z. Kristallogr.* **1974**, *139*, 103.

(14) Phillips, M. L. F.; Harrison, W. T. A.; Gier, T. E.; Stucky, G. D.; Kulkarni, G. V.; Burdett, J. K. *Inorg. Chem.* **1990**, *29*, 2158.

other octahedral substitutions (tin, germanium)^{2,15,16} cause drastic attenuation of powder SHG responses, often by 3 orders of magnitude, relative to KTiOPO_4 . Extraframework cation substitutions for potassium (as MTiOPO_4 , $M = \text{Na, Ag}$) may reduce the SHG response by a similar degree, although the geometry of the Ti/P/O framework remains relatively unchanged.¹⁰ The orthorhombic KTP-type structure is maintained in all these cases, and accurate structural data are essential in order to rationalize the subtle structure-property trends in these materials.

Several theoretical approaches have developed to account for the exceptional nonlinear optical properties of KTiOPO_4 .^{17,18} Here, we use the following simple molecular orbital approach:⁴ The formal $3d^0$ electron configuration of Ti^{IV} in KTiOPO_4 allows oxygen-character valence-band orbitals to be stabilized through mixing of empty metal $d\pi$ orbitals with the oxygen $p\pi$ orbitals. This gain in stabilization energy promotes a distortion of the TiO_6 groups, by shifting the Ti atoms away from the center of their octahedra, toward one of the bridging, inter-Ti oxygen atoms (second-order Jahn-Teller effect).¹⁸ This titanium-atom shift results in an infinite chain of alternatively short and long Ti-O bonds, somewhat analogous to a conjugated chain of carbon atoms. As is also the case with organic molecules and polymers with significant nonlinear optical activity, conjugation permits increased mixing of delocalized charge-transfer excited state (conduction band) character into the ground-state molecular orbitals (valence band), imparting a second-order hyperpolarizability (β_{ijk}) to the ground electronic states.¹⁸ In a noncentrosymmetric lattice like that of KTiOPO_4 , the microscopic β_{ijk} terms cumulatively yield a bulk, observable, second-order susceptibility term, $\chi^{(2)}_{ijk}$, which is in turn responsible for the high SHG response of KTiOPO_4 .

On the basis of this simple MO model, we may qualitatively predict the effect of various atomic substitutions into the KTP structure. The filled $3d^{10}$ electron configuration of Ga^{III} and Ge^{IV} preclude (metal)- $3d\pi$ -(oxygen)- $p\pi$ orbital mixing of the type noted above. Any possible mixing of oxygen $p\pi$ orbitals with the empty, $4d$ -type metal orbitals is likely to be limited, because these latter orbitals are much higher in energy. We note that a small ZrO_6 octahedral distortion and a small SHG response are observed for the KTP analogue CsZrOAsO_4 (formally Zr^{IV} ; $4d^0$).¹⁹ The substitution of fluorine for oxygen will also tend to be deleterious with respect to nonlinear optical behavior. Because the fluorine p orbitals are lower in energy than the corresponding oxygen orbitals, mixing will be less, leading to a larger bandgap, reduction of the second-order hyperpolarizability, β_{ijk} , and reduction in observable SHG response. Structurally, this is likely to be manifested in a reduced octahedral distortion for a $\text{Ga}(\text{O},\text{F})_6$ unit, and a less distinct Ga-(F,O)-Ga short/long bond-length alternation through the structure.

In this paper, we report the syntheses, single-crystal structures, and spectroscopic/optical properties of the KTP-type materials $\text{KGaF}_{1-\delta}(\text{OH})_{\delta}\text{PO}_4$ and $\text{KGa}_{0.5}\text{Ge}_{0.5}(\text{F},\text{OH})_{0.5}\text{O}_{0.5}\text{PO}_4$, in which trivalent gallium substitutes for tetravalent titanium or germanium at the octahedral site. Members of the solid-solution series $\text{KGa}_x\text{Ti}_{1-x}(\text{F},\text{OH})_x\text{O}_{1-x}\text{PO}_4$ have been prepared as powders. $\text{KGaF}_{1-\delta}(\text{OH})_{\delta}\text{PO}_4$ and $\text{KGa}_{0.5}\text{Ge}_{0.5}(\text{F},\text{OH})_{0.5}\text{O}_{0.5}\text{PO}_4$ complement the recently described KGeOPO_4 .²⁰

Experimental Section

Preparation. Single crystals of $\text{KGaF}_{1-\delta}(\text{OH})_{\delta}\text{PO}_4$ were prepared hydrothermally: 0.094 g (1.0 mmol Ga) Ga_2O_3 , 0.30 mL 85% H_3PO_4 , and 0.70 mL 5.00 N KF solution were heat-sealed into a gold tube, dimensions 10 cm long \times 0.64 cm diameter. This gold tube was installed in a Leco Tem-Pres bomb, which was cold pressurized to 1.0 kbar and then heated until a maximum temperature of 700 °C and pressure of \sim 2.5 kbar were reached. The bomb was held at 700 °C for 8 h and then cooled to 525 °C at rate of 2 °C/h, to 300 °C at 10 °C/h, and then cooled to ambient overnight. The tube was reweighed to determine that no leaks occurred during synthesis, reexpanded by briefly heating over a Bunsen burner flame, and opened. The product crystals of $\text{KGaF}_{1-\delta}(\text{OH})_{\delta}\text{PO}_4$ were filtered, rinsed with water, and air dried. Crystals (0.201 g) exceeding 0.1 mm in the maximum linear dimension were recovered. A rhomboidal morphology dominated the transparent crystals, which are stable in air. Pure $\text{KGaF}_{1-\delta}(\text{OH})_{\delta}\text{PO}_4$ could not be made unless the F:Ga ratio in the starting gel was \geq 0.7. Attempts to make KGaFPO_4 via solid-state or anhydrous flux methods did not lead to KTP isostructures (see below).

Single crystals of $\text{KGa}_{0.5}\text{Ge}_{0.5}(\text{F},\text{OH})_{0.5}\text{O}_{0.5}\text{PO}_4$ were prepared from a mixture of 0.047 g (5.1 mmol Ga) of Ga_2O_3 , 0.053 g (5.1 mmol Ge) of GeO_2 , 0.681 g (5.1 mmol P) of KH_2PO_4 , 0.40 mL of 5.00 N KF solution, and 0.10 mL of water. The reactants were sealed into a gold tube and treated by a reaction scheme identical to that used for the $\text{KGaF}_{1-\delta}(\text{OH})_{\delta}\text{PO}_4$ synthesis. After product recovery from the gold tube and workup with water, 0.133 g of air-stable, transparent, rhomboidal crystals of $\text{KGa}_{0.5}\text{Ge}_{0.5}(\text{F},\text{OH})_{0.5}\text{O}_{0.5}\text{PO}_4$ was recovered.

Powders for the series $\text{KGa}_x\text{Ti}_{1-x}(\text{F},\text{OH})_x\text{O}_{1-x}\text{PO}_4$ (KGaTP) were prepared by treating a mixture of Ga_2O_3 and TiCl_4 in the appropriate mole ratio with KH_2PO_4 , KOH , and KF , in water. The synthesis of $\text{KGa}_{0.5}\text{Ti}_{0.5}(\text{F},\text{OH})_{0.5}\text{O}_{0.5}\text{PO}_4$ will serve as an illustrative example: 4.08 g (30 mmol) of KH_2PO_4 was mixed in a Teflon reaction vessel with 1.70 g of 1.82 M (1.25 mmol Ti) TiCl_4 solution, 0.234 g (1.25 mmol Ga) of Ga_2O_3 , 3.64 g of 5.00N KOH solution, and 5.00 mL (5 mmol F) of 1.00 M aqueous KF solution. The resulting hydrogel was shaken well and then autoclaved in water at 200 °C at autogenous pressure for 5 days. The white, powder product was recovered by filtration and washed with water. Powder X-ray measurements (Scintag automated θ - θ diffractometer, $\text{Cu K}\alpha$ radiation, $\lambda = 1.5418 \text{ \AA}$) revealed a pure, crystalline, KTP-type phase, and refined orthorhombic lattice parameters were obtained using Scintag software routines.

Spectroscopic and Optical Measurements. Powder second harmonic generation (PSHG) data for carefully ground and sieved samples, with typical particle sizes in the \sim 5 μm range, were obtained at an incident wavelength of 1064 nm, following the method of Dougherty and Kurtz.²¹ The samples were packed into glass capillary tubes, and data were collected in reflectance mode, using a Spectra-Physics DCR11-3D Nd:YAG laser, which produced 300 mJ, 8 ns pulses at a repetition rate of 2 Hz. Second harmonic light from the samples was collected with an elliptical reflector, separated from the pump beam with a dichroic mirror, and introduced into a grating

(15) Crennell, S. J.; Cheetham, A. K.; Kaduk, J. A.; Jarman, R. H. *J. Mater. Chem.* **1992**, *2*, 785.

(16) Thomas, P. A.; Glazer, A. M.; Watts, B. E. *Acta Crystallogr.* **1990**, *B46*, 333.

(17) Hansen, N. K.; Protas, J.; Marnier, G. C. *R. Acad. Sci., Paris, Ser. II* **1988**, *307*, 475.

(18) Munowitz, M.; Jarman, R. H.; Harrison, J. F. *Chem. Mater.* **1992**, *4*, 1296.

(19) Phillips, M. L. F.; Harrison, W. T. A.; Stucky, G. D. Unpublished work.

(20) Voronkova, V. I.; Yanovskii, V. K.; Sorokina, N. I.; Verin, I. A.; Simonov, V. I. *Crystallogr. Rep.* **1993**, *38*, 662.

(21) Dougherty, J. P.; Kurtz, S. K. *J. Appl. Crystallogr.* **1976**, *9*, 145.

Table 1. Crystallographic Parameters

	KGaF _{1-δ} (OH) _δ PO ₄	KGa _{0.5} Ge _{0.5} (F,OH) _{0.5} O _{0.5} PO ₄
empirical formula	~Ga ₁ K ₁ P ₁ O ₄ F ₁	Ga _{0.5} Ge _{0.5} K ₁ P ₁ O _{4.5} F _{0.5}
formula wt	~222.79	222.73
habit	transparent rhomb	transparent rhomb
crystal system	orthorhombic	orthorhombic
<i>a</i> (Å)	12.717(2)	12.756(2)
<i>b</i> (Å)	6.3021(8)	6.306(1)
<i>c</i> (Å)	10.431(2)	10.413(2)
<i>V</i> (Å ³)	836(2)	838(2)
<i>Z</i>	8	8
space group	<i>Pna</i> 2 ₁ (No. 33)	<i>Pna</i> 2 ₁ (No. 33)
<i>T</i> (°C)	25(2)	25(2)
λ (Mo K α) (Å)	0.71073	0.71073
ρ_{calc} (g/cm ³)	3.54	3.53
μ (Mo K α) (cm ⁻¹)	78.62	81.73
abs corr	analytical	ψ -scan
data limits in <i>hkl</i>	0 ≤ 14, 0 ≤ 9, 0 ≤ 15	0 ≤ 14, 0 ≤ 9, 0 ≤ 15
min, max Δg (e/Å)	-0.84, +0.87	-0.83, +0.87
total data	6313	1622
obsd data ^a	1479	1332
parameters	147	158
<i>R</i> (<i>F</i>) ^b (%)	3.32	3.35
<i>R_w</i> (<i>F</i>) ^c (%)	4.77	3.34

^a $I > 3\sigma(I)$. ^b $R = 100\sum||F_o| - |F_c||/\sum|F_o|$. ^c $R_w = 100[\sum w(|F_o| - |F_c|)^2/\sum w|F_o|^2]^{1/2}$, with w_i as described in the text.

monochromator. The 532 nm light was detected with a Hamamatsu 1P28A photomultiplier tube. Signals from each sample were measured and averaged over 20 shots using a Tektronix 2467B 400 MHz oscilloscope, equipped with a DCS01 digitizing camera system. The resulting PSHG intensities were normalized relative to a reference signal for KTiOPO₄.

UV/visible spectra were collected in hemispherical reflectance mode using an automated Cary 14 UV-visible-IR spectrometer. Thermogravimetric (TGA) data were collected on a DuPont 9900 system. ¹H MAS NMR data for KGaF_{1-δ}(OH)_δPO₄ were collected on a General Electric GN-300 spectrometer, using a Chemagnetics probe.

Structure Determination. A transparent, well-faceted, single crystal of KGaF_{1-δ}(OH)_δPO₄ (rhombic, dimensions ca. 0.4 × 0.3 × 0.3 mm) was mounted on a thin glass fiber with epoxy. Room-temperature [25(1)°C] intensity data were collected on a Huber automated 4-circle diffractometer (graphite-monochromated Mo K α radiation, $\lambda = 0.71073$ Å), as outlined in Table 1 (cell parameters from 25 centered, strong reflections; θ - 2θ scan mode; $2\theta_{\text{max}} = 65^\circ$; 6313 reflections scanned; complete hemisphere of data). Optimal values of *F* and $\sigma(F)$ were extracted by profile fitting,²² and an analytical absorption correction²³ (transmission-factor range 0.025–0.258) was also applied during data reduction, resulting in 1479 observed reflections [$I > 3\sigma(I)$] after merging non-Friedel equivalences. Systematic absences in the reduced data (00*l*, $l \neq 2n$; *h*0*l*, $h \neq 2n$; 0*kl*, $h + l \neq 2n$) were consistent with space groups *Pna*2₁ (No. 33) or *Pnam* (nonstandard setting of *Pnma*, No. 62). The nonzero PSHG response of KGaF_{1-δ}(OH)_δPO₄ indicated that space group *Pna*2₁ was the correct one.

The KGa_{0.5}Ge_{0.5}(F,OH)_{0.5}O_{0.5}PO₄ data collection was performed in similar style, as summarized in Table 1. Systematic absences indicated space groups *Pna*2₁ or *Pnam*, and 1332 observed data with $I > 3\sigma(I)$ were used in the structure refinement. The nonzero PSHG response for KGa_{0.5}Ge_{0.5}(F,OH)_{0.5}O_{0.5}PO₄ indicated space group *Pna*2₁.

The structure of KGaF_{1-δ}(OH)_δPO₄ was refined in space group *Pna*2₁ (No. 33), using the atomic coordinates of KVOPO₄¹⁴ as a starting model, with Ga substituting for V, and all 10 oxygen sites initially fully occupied by O. The refinement converged smoothly, without any indications of serious pseudosymmetry.¹⁶ After anisotropic refinement, satisfactory residuals of $R = 3.67\%$, and $R_w = 5.85\%$ were obtained, but the thermal parameters for O(9) and O(10), the atoms linking the

octahedral gallium atoms into infinite chains, refined to anomalously low values ($U_{\text{eq}}[\text{O}(9)] \approx 0.004 \text{ \AA}^2$, $U_{\text{eq}}[\text{O}(10)] \approx -0.001 \text{ \AA}^2$) compared to the other eight oxygen atoms (average $U_{\text{eq}} \approx 0.012 \text{ \AA}^2$).

Further refinement cycles, which allowed for various fluorine-atom occupancy models of the O(9) and O(10) sites were thus carried out. A refinement that assumed full fluorine atom occupancy of the O(9) and O(10) sites converged at lower residuals of $R = 3.32\%$ and $R_w = 4.77\%$, and the F(9) and F(10) equivalent isotropic thermal parameters refined to more reasonable values [$\sim 0.013 \text{ \AA}^2$ and 0.012 \AA^2 for F(9) and F(10), respectively].

A model that assumed a fixed 70:30 F:OH occupancy of both the O(9) and O(10) sites (see below) converged to very similar residuals to the all-F model: $R = 3.36\%$; $R_w = 4.92\%$, and with similar equivalent isotropic thermal factors for the F/O(9) and F/O(10) sites. Finally, a refinement which allowed the F:O content of both sites to vary independently, subject to the constraint that $\text{occ}(\text{O}) + \text{occ}(\text{F}) = 1.00$, was attempted. This refinement suggested that $\geq 95\%$ of each site was occupied by F. Because of the relative lack of sensitivity of the refinement to the precise F/O ratio, the F/O(9) and F/O(10) sites were modeled as fluorine atoms only in the final refinement cycles, which were against *F* and included anisotropic temperature factors for all atoms and a Larson-type secondary extinction correction.²⁴ All of these models led to very similar refined framework geometries (see below).

The least-squares and subsidiary calculations were performed using the Oxford CRYSTALS²⁵ system running on a DEC MicroVAX-3100 computer. Complex, neutral-atom scattering factors were obtained from the *International Tables*.²⁶ Final residuals, as defined in Table 1, were $R = 3.32\%$ and $R_w = 4.77\%$ ($w_i = 1/\sigma_i^2$) for 147 parameters.

Refinement of the KGa_{0.5}Ge_{0.5}(F,OH)_{0.5}O_{0.5}PO₄ structure followed the same procedure, using the KGaF_{1-δ}(OH)_δPO₄ atomic coordinates (space group *Pna*2₁) as a starting model, with Ga and Ge assumed to randomly occupy both octahedral sites. The initial refinement cycles converged successfully, but refinement schemes that attempted to vary the Ga and Ge site occupancies [subject to the constraint of $\text{occ}(\text{Ga}) + \text{occ}(\text{Ge}) = 1$] did not show any significant degree of Ga/Ge ordering over the two octahedral sites. Since the scattering factors of Ga and Ge are so similar with respect to X-rays, this result, which shows no preferential Ga/Ge site occupancies, should be regarded with appropriate caution. However, consideration of average octahedral bond distances and bond valence sum calculations support the assumption of Ga/Ge disorder (vide infra). Constrained site-occupancy refinements for F and O over the O/F(9) and O/F(10) showed no indication of preferential occupancy for either sites, and the final cycles of least-squares modeled both sites as 50% F and 50% O.

At the $R \approx 5\%$ stage, difference Fourier maps revealed two significant electron density maxima in the extraframework channels, each displaced by ~ 1.4 Å from the K(1) and K(2) sites, respectively. A refinement was carried out that modeled these two additional sites as potassium cations (positions, site occupancies, isotropic thermal parameters refined), along with position/site occupancy/anisotropic thermal parameter variation for K(1) and K(2). Positional and U_{ij} values for the other atoms were also varied. This model rapidly converged, with both the additional K sites refining to chemically significant occupancies. Although the isotropic thermal parameters for these two sites, K(11) and K(12), refined to rather small values, it is striking, that *without occupancy constraints*, the K(1) and K(11) fractional site occupancies [0.79(1) and 0.213(9), respectively] add up to unity (1.00), as do the K(2) [0.88(1)] and K(12) [0.117(9)] occupancies [sum = 1.00]. Both K(11) and K(12) have reasonable geometrical parameters, as described below. Final residuals of $R = 3.35\%$ and $R_w = 3.34\%$ (Tukey-Prince

(24) Larson, A. C. *Acta Crystallogr.* **1967**, *23*, 664.

(25) Watkin, D. J.; Carruthers, J. R.; Betteridge, P. W. *CRYSTALS User Guide*, Chemical Crystallography Laboratory, Oxford University, UK, 1990.

(26) *International Tables for X-Ray Crystallography*; Kynoch Press: Birmingham, 1974; Volume IV, Table 2.3.1.

(22) Lehmann, M. S.; Larsen, F. K. *Acta Crystallogr.* **1974**, *A30*, 580.

(23) Busing, W. R.; Levy, H. A. *Acta Crystallogr.* **1957**, *10*, 180.

type w_i , fitted using a two-term Chebychev polynomial²⁷) resulted for 158 variable parameters (Table 1).

Results

Composition of $\text{KGaF}_{1-\delta}(\text{OH})_{\delta}\text{PO}_4$. One question not unambiguously answered by the single-crystal refinement of $\text{KGaF}_{1-\delta}(\text{OH})_{\delta}\text{PO}_4$ is the precise atomic composition of this phase, in terms of fluoride versus hydroxide content. It is clear from the various single-crystal refinements carried out (vide supra) that $\text{KGaF}_{1-\delta}(\text{OH})_{\delta}\text{PO}_4$ contains a substantial amount of F^- ions substituting at the O(9) and O(10) atomic sites and that this phase cannot be formulated as KGaOHPO_4 . However, as noted above, there appear to be quite strict requirements, in terms of the fluorine:gallium atomic ratio, for $\text{KGaF}_{1-\delta}(\text{OH})_{\delta}\text{PO}_4$ to form as a pure phase; in particular, pure $\text{KGaF}_{1-\delta}(\text{OH})_{\delta}\text{PO}_4$ will not form if the F:Ga ratio falls below about 0.7:1.0. For F:Ga ratios below 0.7, unknown (by powder X-ray diffraction) impurity phases are formed, in addition to $\text{KGaF}_{1-\delta}(\text{OH})_{\delta}\text{PO}_4$. KGaFPO_4 has not been synthesized from a solid-state reaction (stoichiometric quantities of Ga_2O_3 , KF , and $\text{NH}_4\text{H}_2\text{PO}_4$) nor from an anhydrous melt (KPO_3 , Ga_2O_3 , and KF). Thus, it is tempting to speculate that $\text{KGaF}_{1-\delta}(\text{OH})_{\delta}\text{PO}_4$ will only form in the presence of both fluoride and (precursors of) hydroxide ions, and for convenience here, the formula is expressed as $\text{KGaF}_{1-\delta}(\text{OH})_{\delta}\text{PO}_4$, with $\delta \approx 0.3$. This conjecture is supported by other measurements, as follows.

Although the single-crystal refinement is insensitive to the exact fluoride/hydroxide content in $\text{KGaF}_{1-\delta}(\text{OH})_{\delta}\text{PO}_4$, a measure of this can be obtained from the TGA results. Crystals of $\text{KGaF}_{1-\delta}(\text{OH})_{\delta}\text{PO}_4$, from the same batch from which the crystal used for structure determination was selected, were thoroughly ground. After slight loss of surface moisture below 50 °C, the thermogram showed negligible weight loss up to ~530 °C and then a sharp 1.1% weight loss, complete by 620 °C. A very small (<0.4%) additional weight loss occurred by 1000 °C. This first weight loss is very unlikely to correspond to expulsion of bound water at ~530 °C and is presumably due to water loss resulting from the decomposing hydroxide (Ga–OH–Ga) group. This weight loss corresponds to a formulation of $\sim\text{KGaF}_{0.7}(\text{OH})_{0.3}\text{PO}_4$, in good agreement with the F:OH ratio implied by the synthesis conditions (F:Ga ratio ~0.7:1.0). Elemental analysis (Galbraith Laboratories, Knoxville, TN) for $\text{KGaF}_{1-\delta}(\text{OH})_{\delta}\text{PO}_4$ yielded a hydrogen content of 0.1 wt %, corresponding to $\sim\text{KGaF}_{0.78}(\text{OH})_{0.22}\text{PO}_4$, although the uncertainty on this derived stoichiometry is high. Additional evidence for some incorporated hydroxide in $\text{KGaF}_{1-\delta}(\text{OH})_{\delta}\text{PO}_4$ comes from ¹H MAS NMR data.⁹ A single, weak, broad peak was observed, shifted downfield by 5.27 ppm from a reference signal for hydroxyapatite. This chemical shift could be due to either OH or H₂O, but the weak signal and lack of spinning sidebands probably indicates a hydroxide group, rather than H₂O.²⁸ The $\text{KGa}_x\text{Ti}_{1-x}(\text{F},\text{OH})_x\text{O}_{1-x}\text{PO}_4$ solid solution members (vide infra) also appear to contain a consistent F:Ga ratio <1, based on elemental analysis data.

Table 2. Atomic Positional/Thermal Parameters for $\text{KGaF}_{1-\delta}(\text{OH})_{\delta}\text{PO}_4$

atom	x	y	z	U_{eq}^a
K(1)	0.3814(1)	0.7766(2)	0.3192(2)	0.0223
K(2)	0.1042(1)	0.6926(3)	0.0744(2)	0.0227
Ga(1)	0.38786(3)	0.49584(8)	0.0146(2)	0.0085
Ga(2)	0.24667(4)	0.25194(9)	0.2637(2)	0.0085
P(1)	0.49995(8)	0.3275(2)	0.2643(2)	0.0086
P(2)	0.18362(8)	0.5006(2)	0.5149(2)	0.0085
O(1)	0.4860(4)	0.4818(8)	0.1514(5)	0.0121
O(2)	0.5110(4)	0.4678(9)	0.3835(4)	0.0109
O(3)	0.4007(3)	0.1905(6)	0.2810(5)	0.0113
O(4)	0.5963(3)	0.1857(6)	0.2448(4)	0.0124
O(5)	0.1140(3)	0.3094(6)	0.5454(4)	0.0124
O(6)	0.1139(3)	0.6929(6)	0.4858(5)	0.0130
O(7)	0.2573(3)	0.5432(8)	0.6311(5)	0.0120
O(8)	0.2571(3)	0.4538(8)	0.4014(5)	0.0125
F(9)	0.2729(4)	0.4788(6)	0.1422(4)	0.0127
F(10)	0.2282(3)	0.0272(7)	0.3920(4)	0.0114

$$^a U_{\text{eq}} (\text{\AA}^2) = (U_1 U_2 U_3)^{1/3}.$$

Table 3. Selected Geometrical Data (angstroms, degrees) for $\text{KGaF}_{1-\delta}(\text{OH})_{\delta}\text{PO}_4$

K(1)–O(1)	2.878(6)	K(1)–O(2)	2.637(5)
K(1)–O(3)	2.650(4)	K(1)–O(5)	2.864(5)
K(1)–O(7)	3.127(5)	K(1)–O(8)	2.716(5)
K(1)–F(9)	2.972(5)	K(1)–F(10)	2.621(4)
K(2)–O(1)	2.668(5)	K(2)–O(2)	3.019(6)
K(2)–O(3)	3.061(5)	K(2)–O(4)	2.975(4)
K(2)–O(5)	2.791(4)	K(2)–O(7)	2.887(5)
K(2)–O(8)	3.013(5)	K(2)–F(9)	2.630(5)
K(2)–F(10)	3.042(5)		
Ga(1)–O(1)	1.897(5)	Ga(1)–O(2)	1.891(5)
Ga(1)–O(5)	2.002(4)	Ga(1)–O(6)	1.933(4)
Ga(1)–F(9)	1.980(4)	Ga(1)–F(10)	1.963(4)
Ga(2)–O(3)	2.005(3)	Ga(2)–O(4)	1.962(3)
Ga(2)–O(7)	1.909(5)	Ga(2)–O(8)	1.923(5)
Ga(2)–F(9)	1.939(4)	Ga(2)–F(10)	1.963(4)
P(1)–O(1)	1.538(6)	P(1)–O(2)	1.532(5)
P(1)–O(3)	1.539(4)	P(1)–O(4)	1.530(4)
P(2)–O(5)	1.529(4)	P(2)–O(6)	1.532(4)
P(2)–O(7)	1.555(5)	P(2)–O(8)	1.537(5)
F(9)–Ga(1)–F(10)	83.6(1)	F(9)–Ga(2)–F(10)	176.5(2)
Ga(1)–F(9)–Ga(2)	127.3(2)	Ga(1)–F(10)–Ga(2)	127.4(2)

Structure of $\text{KGaF}_{1-\delta}(\text{OH})_{\delta}\text{PO}_4$. Final atomic positional and equivalent isotropic thermal parameters for $\text{KGaF}_{1-\delta}(\text{OH})_{\delta}\text{PO}_4$ are listed in Table 2, with selected bond distance/angle data in Table 3. $\text{KGaF}_{1-\delta}(\text{OH})_{\delta}\text{PO}_4$ crystallizes as a typical orthorhombic $Pna2_1$ KTP-type material,^{2,13} with gallium replacing titanium at the two octahedral sites and fluorine selectively substituting for 2 of the 10 distinct oxygen atoms. The $\text{KGaF}_{1-\delta}(\text{OH})_{\delta}\text{PO}_4$ structure is built up from vertex-linked $\text{Ga}(\text{O},\text{F})_6$ octahedra and PO_4 tetrahedra, connected via Ga–(F/OH)–Ga and Ga–O–P bonds.²

Both potassium cations in $\text{KGaF}_{1-\delta}(\text{OH})_{\delta}\text{PO}_4$, which occupy “extraframework” sites in the corrugated [001] channels, adopt irregular coordination, at sites very similar to their counterparts in KTiOPO_4 . The K(1) site is 8-coordinate to nearby O and F atoms, with a $d_{\text{av}}(\text{K}(1)\text{–O},\text{F})$ of 2.808(2) Å. A Brese–O’Keeffe bond valence sum²⁹ (BVS) value of 1.29 results for this cation, taking into account the differently parametrized K–O and K–F bonds. K(2) is 9-coordinate, with $d_{\text{av}}(\text{K}(2)\text{–O},\text{F}) = 2.898(2)$ Å, $\text{BVS}[\text{K}(2)] = 1.12$. Neither of these potassium-ion geometries approaches any type of regular polyhedron, and in both cases, the potassium ion is grossly shifted from the geometrical center of its oxygen-

(27) Carruthers, J. R.; Watkin, D. J. *Acta Crystallogr.* **1979**, *A35*, 698.

(28) Yesinowski, J. P.; Eckert, H.; Rossman, G. R. *J. Am. Chem. Soc.* **1988**, *110*, 1367.

(29) Brese, N. E.; O’Keeffe, M. *Acta Crystallogr.* **1991**, *B47*, 192.

Table 4. Atomic Positional/Thermal Parameters for KGa_{0.5}Ge_{0.5}(F,OH)_{0.5}O_{0.5}PO₄

atom	x	y	z	U _{eq} ^a	occ ^b
K(1)	0.3848(3)	0.7799(6)	0.3262(4)	0.0407	0.79(1)
K(2)	0.1029(3)	0.6923(6)	0.0781(4)	0.0423	0.88(1)
K(11)	0.901(1)	0.687(2)	0.454(1)	0.019(3) ^c	0.213(9)
K(12)	0.119(1)	0.725(2)	0.209(1)	0.007(3) ^c	0.117(9)
Ga(1)	0.38638(5)	0.4986(2)	0.0118(3)	0.0158	
Ga(2)	0.24805(8)	0.2514(2)	0.2615(2)	0.0163	
P(1)	0.5001(2)	0.3277(2)	0.2648(5)	0.0144	
P(2)	0.1835(1)	0.5009(4)	0.5137(5)	0.0140	
O(1)	0.4865(9)	0.480(2)	0.1504(8)	0.0165	
O(2)	0.5133(9)	0.468(2)	0.3843(8)	0.0222	
O(3)	0.4016(5)	0.189(1)	0.2845(9)	0.0179	
O(4)	0.5965(5)	0.186(1)	0.2467(8)	0.0169	
O(5)	0.1154(6)	0.309(1)	0.5465(7)	0.0163	
O(6)	0.1128(7)	0.694(1)	0.4874(8)	0.0200	
O(7)	0.2576(9)	0.546(2)	0.6289(9)	0.0195	
O(8)	0.2568(9)	0.455(2)	0.3994(9)	0.0177	
O(9)	0.273(1)	0.481(1)	0.1420(7)	0.0162	
O(10)	0.226(1)	0.028(2)	0.3902(7)	0.0172	

^a U_{eq}(Å²) = (U₁U₂U₃)^{1/3}. ^b Fractional site occupancy. ^c U_{iso} (Å²).

atom neighbors, by 0.94 Å in the case of K(1), and 1.09 Å in the case of K(2). For both potassium sites, this shift, from the centroid of their O atom neighbors, is largely in the crystallographic z direction, i.e., along the polar axis. The BVS value for K(1) is somewhat larger than the ideal value of 1.00 expected for K⁺, and a similar effect is observed in other KTP analogues such as K_{0.42}Na_{0.58}TiOPO₄.³⁰ Despite this large BVS value for K(1), both the K(1) and K(2) cations are easily ion-exchangeable under moderate conditions,^{2,10} and guest cation movement along the polar axis direction plays an important role in the ferroelectric → paraelectric phase transition (space group transition *Pna*2₁ → *Pnan*) in KTP-type phases^{16,31–33} and in also in domain-inversion and twinning processes in KTP-type structures.¹²

The two distinct gallium sites in KGaF_{1-δ}(OH)_δPO₄ are both octahedral (Figure 1), but both the Ga(1)O₄F₂ and Ga(2)O₄F₂ groups are much less distorted than the corresponding Ti(1)O₆ and Ti(2)O₆ groups in titanium-containing KTP congeners. In particular, KGaF_{1-δ}(OH)_δPO₄ lacks any short “double” Ga=F bonds, equivalent to the “titanyl” Ti=O bonds (or [TiO]²⁺ units) in KTiOPO₄. The average gallium to oxygen/fluorine bond distances in KGaF_{1-δ}(OH)_δPO₄ [*d*_{av}(Ga(1)–O,F) = 1.944(2) Å, *d*_{av}(Ga(2)–O,F) = 1.950(2) Å] accord well with the bond distances expected for these species on the basis of ionic radii sums.³⁴ BVS values²⁹ for Ga(1) (3.12) and Ga(2) (3.04) are commensurate with those expected for trivalent gallium. Both tetrahedral phosphorus atom sites in KGaF_{1-δ}(OH)_δPO₄ are typical, with average P–O distances of 1.535(3) Å for P(1)O₄ (BVS = 4.82) and 1.538(3) Å for P(2)O₄ (BVS = 4.77), respectively.

Structure of KGa_{0.5}Ge_{0.5}(F,OH)_{0.5}O_{0.5}PO₄. Final atomic positional and equivalent isotropic thermal parameters for KGaF_{1-δ}(OH)_δPO₄ are listed in Table 4, with selected bond distance/angle data in Table 5.

Table 5. Selected Bond Distances/Angles for KGa_{0.35}Ge_{0.5}(F,OH)_{0.5}O_{0.5}PO₄

K(1)–O(1)	2.93(1)	K(1)–O(2)	2.63(1)
K(1)–O(3)	2.626(8)	K(1)–O(5)	2.918(8)
K(1)–O(7)	3.22(1)	K(1)–O(8)	2.73(1)
K(1)–O(9)	3.05(1)	K(1)–O(10)	2.64(1)
K(2)–O(1)	2.66(1)	K(2)–O(2)	3.05(1)
K(2)–O(3)	3.058(9)	K(2)–O(4)	2.965(8)
K(2)–O(5)	2.80(1)	K(2)–O(7)	2.90(1)
K(2)–O(8)	3.07(1)	K(2)–O(9)	2.63(1)
K(2)–O(10)	3.11(1)		
K(11)–O(1)	3.10(2)	K(11)–O(2)	2.70(2)
K(11)–O(3)	2.96(1)	K(11)–O(4)	3.04(1)
K(11)–O(6)	2.72(2)	K(11)–O(7)	3.08(2)
K(11)–O(8)	2.97(2)	K(11)–O(9)	3.14(2)
K(11)–O(10)	2.70(2)		
K(12)–O(1)	2.58(2)	K(12)–O(2)	2.98(2)
K(12)–O(4)	2.64(2)	K(12)–O(6)	2.90(2)
K(12)–O(7)	2.70(2)	K(12)–O(8)	3.15(2)
K(12)–O(9)	2.60(2)	K(12)–O(10)	3.01(2)
K(1)···K(11) ^a	1.37(1)	K(2)···K(12) ^a	1.40(1)
Ga(1)–O(1)	1.931(9)	Ga(1)–O(2)	1.86(1)
Ga(1)–O(5)	1.988(7)	Ga(1)–O(6)	1.937(8)
Ga(1)–O(9)	1.99(1)	Ga(1)–O(10)	1.92(1)
Ga(2)–O(3)	2.011(7)	Ga(2)–O(4)	1.978(7)
Ga(2)–O(7)	1.89(1)	Ga(2)–O(8)	1.93(1)
Ga(2)–O(9)	1.933(8)	Ga(2)–O(10)	1.964(9)
P(1)–O(1)	1.54(1)	P(1)–O(2)	1.54(1)
P(1)–O(3)	1.544(7)	P(1)–O(4)	1.530(7)
P(2)–O(5)	1.530(8)	P(2)–O(6)	1.540(8)
P(2)–O(7)	1.55(1)	P(2)–O(8)	1.54(1)
O(9)–Ga(1)–O(10)	84.8(2)	O(9)–Ga(2)–O(10)	176.9(5)
Ga(1)–O(9)–Ga(2)	126.9(6)	Ga(1)–O(10)–Ga(2)	128.6(7)

^a Apparent contact due to disorder (see text).

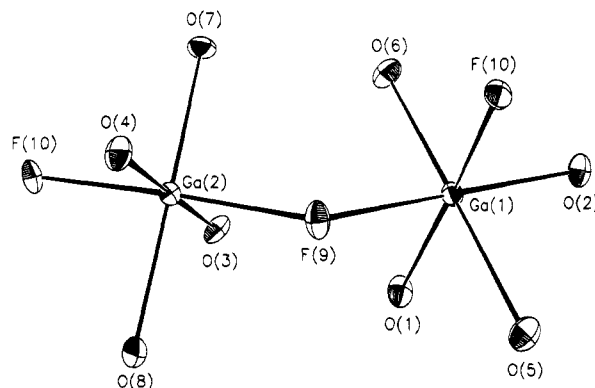


Figure 1. Detail of the gallium atom geometry in the KGaF_{1-δ}(OH)_δPO₄, showing the infinite chain of Ga–F–Ga bonds linking the octahedral centers. The F(9) and F(10) centers also have a small hydroxide (oxygen atom) content: see text.

The octahedral Ga/Ge sites (Figure 2) in KGa_{0.5}Ge_{0.5}(F,OH)_{0.5}O_{0.5}PO₄ are fairly regular, with *d*_{av}(Ga/Ge(1)–O,F) = 1.938(4) Å, and *d*_{av}(Ga/Ge(2)–O,F) = 1.951(4) Å. As with KGaF_{1-δ}(OH)_δPO₄, there are no identifiable short bonds (*d* < 1.75 Å) in the octahedral chains, although fluorine and oxygen are apparently disordered over the O/F(9) and O/F(10) sites in this phase. Bond valence sums²⁹ for the two octahedral sites, using parameters appropriate to Ga^{III} yielded the following: BVS[Ga/Ge(1)] = 3.61, BVS[Ga/Ge(2)] = 3.48. Using parameters appropriate to Ge^{IV} gave BVS[Ga/Ge(1)] = 3.44 and BVS[Ga/Ge(2)] = 3.32. Both of these calculations suggest partial Ga/Ge occupancy of both sites, consistent with the X-ray Ga/Ge refinements described above. The two phosphate tetrahedra in KGa_{0.5}Ge_{0.5}(F,OH)_{0.5}O_{0.5}PO₄ [*d*_{av}(P(1)–O) = 1.539(5) Å,

(30) Crennell, S. J.; Morris, R. E.; Cheetham, A. K.; Jarman, R. H. *Chem. Mater.* **1992**, *4*, 82.

(31) Northrup, P. A.; Parise, J. B.; Cheng, L. K.; Cheng, L. T.; McCarron, E. M. *Chem. Mater.* **1994**, *6*, 434.

(32) Harrison, W. T. A.; Gier, T. E.; Stucky, G. D.; Schultz, A. J. *J. Chem. Soc., Chem. Comm.* **1990**, 540.

(33) Yanovskii, V. K.; Voronkova, V. I. *Phys. Status Solidi* **1980**, *93*, 665.

(34) Shannon, R. D. *Acta Crystallogr.* **1976**, *A32*, 751.

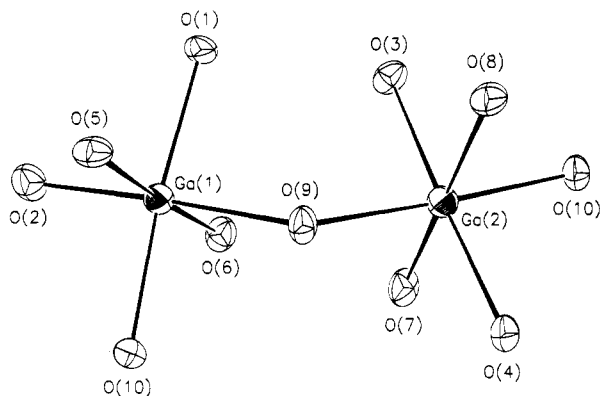


Figure 2. Gallium-germanium/oxygen-atom geometry in $\text{KGa}_{0.5}\text{Ge}_{0.5}(\text{F},\text{OH})_{0.5}\text{O}_{0.5}\text{PO}_4$, showing the infinite connectivity linking the octahedral centers, via O/F(9) and O/F(10).

$\text{BVS}[\text{P}(1)] = 4.78$; $d_{\text{av}}(\text{P}(2)-\text{O}) = 1.540(5) \text{ \AA}$, $\text{BVS}[\text{P}(2)] = 4.76$ are typical.

The most interesting structural feature of $\text{KGa}_{0.5}\text{Ge}_{0.5}(\text{F},\text{OH})_{0.5}\text{O}_{0.5}\text{PO}_4$ concerns the partially disordered potassium species. K(1) and K(2) occupy similar sites to their counterparts in $\text{KGaF}_{1-\delta}(\text{OH})_{\delta}\text{PO}_4$ and KTiOPO_4 . K(1) [$d_{\text{av}} = 2.843(8) \text{ \AA}$, $\text{BVS} = 1.34$] is 8-coordinate, and K(2) [$d_{\text{av}} = 2.92(1) \text{ \AA}$, $\text{BVS} = 1.20$] is 9-coordinate. Both these coordinations are irregular and displaced from the centroid of their O/F-atom neighbors [by $\Delta = 1.03 \text{ \AA}$ for K(1); by $\Delta = 0.73 \text{ \AA}$ for K(2)], as was the case for the two K sites in $\text{KGaF}_{1-\delta}(\text{OH})_{\delta}\text{PO}_4$. K(11), the near-neighbor site to K(1) (Table 5) is 9-coordinate to nearby O/F atoms, with $d_{\text{av}} = 2.934(7) \text{ \AA}$, and $\text{BVS} = 1.14$. K(12), the disordered partner of K(2), is 8-coordinate, with $d_{\text{av}} = 2.820(8) \text{ \AA}$, and $\text{BVS} = 1.42$. Both K(11) ($\Delta = 0.76 \text{ \AA}$) and K(12) ($\Delta = 0.97 \text{ \AA}$) are also grossly displaced from the centroids of their oxygen-atom neighbors. The existence of these K(11) and K(12) sites has been predicted by Thomas and Glazer in their study of twinning and domain inversion processes in KTP-type structures.¹² These authors termed these two locations as "hole" sites, denoted $h(1)$ and $h(2)$, and described their significance with respect to ionic diffusion and ion-exchange in KTP phases. A recent single-crystal study of *ion-exchanged* $\text{K}_{0.84}\text{Rb}_{0.16}\text{TiOPO}_4$ by Thomas et al.³⁵ revealed a low [0.038(3)] fractional site occupancy of the $h(1)$ site by rubidium, but no other crystal-structure studies of KTP-type phases have indicated any simultaneous occupancy of both the "normal" [K(1) and K(2)] and hole [$h(1)$ and $h(2)$] sites.

$\text{KGa}_x\text{Ti}_{1-x}(\text{F},\text{OH})_x\text{O}_{1-x}\text{PO}_4$ Solid Solution. The complete solid solution range between KTiOPO_4 and $\text{KGaF}_{1-\delta}(\text{OH})_{\delta}\text{PO}_4$ was successfully prepared, according to the hydrothermal methods outlined above, leading to white powders in all cases. The fluorine content of four members of the series was established by elemental analysis: for $\text{KGa}_x\text{Ti}_{1-x}(\text{F},\text{OH})_x\text{O}_{1-x}\text{PO}_4$ with $x = 0.2$, the F:Ga ratio was 0.74:1.00. For $x = 0.4, 0.6$, and 0.8 , comparable ratio values of 0.58:1.00, 0.76:1.00, and 0.69:1.00, respectively, were obtained. We estimate that the error on these values is $\pm 5\%$. Thus, the F:Ga ratio in these phases appears to be a fairly consistent 0.7:1.0 across the entire $\text{KGa}_x\text{Ti}_{1-x}(\text{F},\text{OH})_x\text{O}_{1-x}\text{PO}_4$ series. This same F:Ga ratio is also found for $\text{KGaF}_{1-\delta}(\text{OH})_{\delta}\text{PO}_4$ itself, suggesting that a particular F:OH distribution

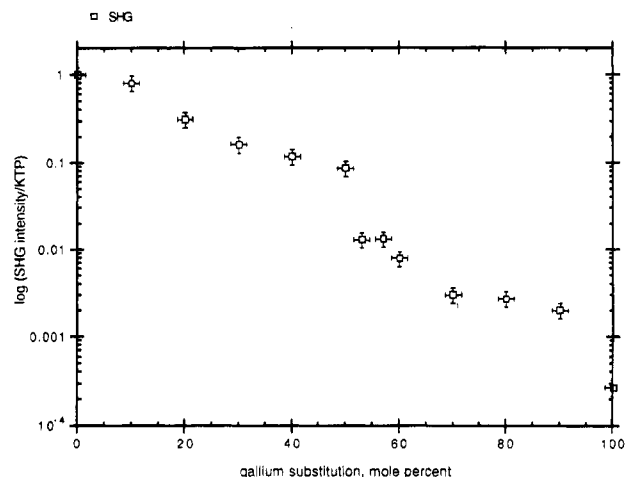


Figure 3. Plot of powder SHG response versus percentage gallium composition for the series $\text{KGa}_x\text{Ti}_{1-x}(\text{F},\text{OH})_x\text{O}_{1-x}\text{PO}_4$.

over the O(9) and O(10) interoctahedral bridging sites is a characteristic feature of these KTP-type phases containing gallium.

The trends in decreasing orthorhombic a , b , and c unit-cell dimensions and unit-cell volume are approximately linear with increasing x for the $\text{KGa}_x\text{Ti}_{1-x}(\text{F},\text{OH})_x\text{O}_{1-x}\text{PO}_4$ series (Vegard's law obeyed). The unit cell volume of $\text{KGaF}_{1-\delta}(\text{OH})_{\delta}\text{PO}_4$, 837.1 \AA^3 , has decreased by about 3.9%, compared to that of KTiOPO_4 (870.9 \AA^3). This trend is not commensurate with differences in cationic radii,³⁴ as the values for octahedral Ti^{IV} ($r = 0.745 \text{ \AA}$) and Ga^{III} ($r = 0.76 \text{ \AA}$) are almost identical. This trend could be due to F^- ($r = 1.145 \text{ \AA}$) and OH^- ($r = 1.18 \text{ \AA}$) progressively replacing the slightly larger O^{2-} ($r = 1.21 \text{ \AA}$) at the O(9) and O(10) sites. Conversely, the powder SHG responses³⁶ of the various members of the $\text{KGa}_x\text{Ti}_{1-x}(\text{F},\text{OH})_x\text{O}_{1-x}\text{PO}_4$ series, plotted in Figure 3 as a function of Ga content, show a highly nonlinear dependence on x : A steady decline in powder SHG is observed for samples with less than 50% Ga incorporated, relative to the powder SHG response of KTiOPO_4 itself ($600 \times$ quartz). A distinct break occurs between 50% and 53% Ga substitution, corresponding to a nearly 10-fold drop in SHG intensity. Another fairly smooth decrease in SHG intensity then ensues, down to the minimal response of $\text{KGaF}_{1-\delta}(\text{OH})_{\delta}\text{PO}_4$ itself ($\sim 0.2 \times$ quartz). The reason for this variation of powder SHG with respect to Ga/Ti composition is not yet understood.

Spectroscopic Data. UV/visible spectra for various KTP-type phases are shown in Figure 4. The estimated bandgap for KTiOPO_4 is 350 nm (3.5 eV), and comparable values of 300 nm (4.1 eV) for CsZrOAsO_4 , 270 nm (4.6 eV) for $\text{KGaF}_{1-\delta}(\text{OH})_{\delta}\text{PO}_4$, and 225 nm (5.5 eV) for KSnOPO_4 result. KTiOPO_4 has a powder SHG of $\sim 600 \times$ quartz, while CsZrOAsO_4 , $\text{KGaF}_{1-\delta}(\text{OH})_{\delta}\text{PO}_4$, and KSnOPO_4 all have small powder SHG responses, no more than $10 \times$ quartz. Despite their small magnitudes, it is notable that the trend of SHG values for these three phases ($\text{CsZrOAsO}_4 > \text{KGaF}_{1-\delta}(\text{OH})_{\delta}\text{PO}_4 > \text{KSnOPO}_4$) is the reverse of the order of increasing bandgaps.

(35) Thomas, P. A.; Duhlev, R.; Teat, S. J. *Acta Crystallogr.* **1994**, *B50*, 538.

(36) Phillips, M. L. F.; Harrison, W. T. A.; Gier, T. E.; Stucky, G. D. *Proc. SPIE* **1989**, *1104*, 225-231.

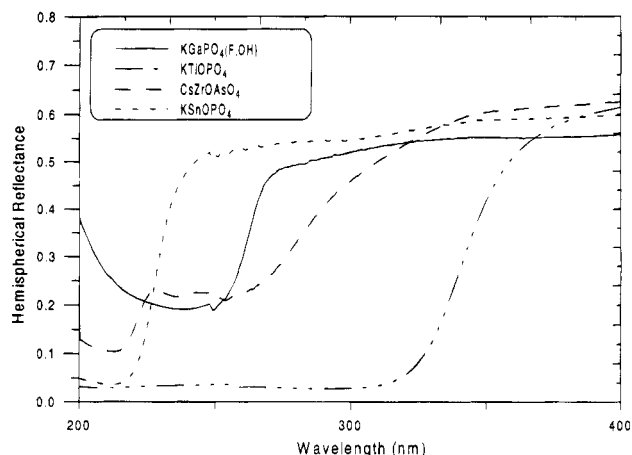


Figure 4. Plot of UV/visible spectra for various KTP isostructures (see text).

Discussion

$\text{KGaF}_{1-\delta}(\text{OH})_{\delta}\text{PO}_4$ and $\text{KGa}_{0.5}\text{Ge}_{0.5}(\text{F},\text{OH})_{0.5}\text{O}_{0.5}\text{PO}_4$ have been prepared as single crystals and structurally and optically characterized. They adopt typical KTP-type $Pna2_1$ orthorhombic structures, but without the characteristic M -O short-long bond-length alternation in the octahedral chain, as found for KTiOPO_4 and other titanium-containing congeners. As seen in other KTP isostructures in which octahedral MO_6 distortion is reduced, the strong optical nonlinearity characteristic of KTiOPO_4 is lost. This is consistent with the phenomenological requirement for a short $\text{Ti}=\text{O}$ (formal metal electron configuration $3d^0$) or $\text{V}=\text{O}$ ($3d^1$) bond to be present in the KTP structure for a large SHG response to be observed.^{2,10,14}

The qualitative predictions of the molecular orbital argument outlined in the introduction have been borne out by $\text{KGaF}_{1-\delta}(\text{OH})_{\delta}\text{PO}_4$. Specifically, by raising the energy of the charge-transfer band (predominant Ga 4d character, compared to 3d character for Ti), and lowering the energy of the valence-band orbitals (F substituting for O), the mixing of the metal $d\pi$ and anionic $p\pi$ orbitals is inhibited. The bandgap is increased, compared to that of KTiOPO_4 , as observed in the UV/visible spectrum of $\text{KGaF}_{1-\delta}(\text{OH})_{\delta}\text{PO}_4$. Structurally, the magnitude of the second-order Jahn-Teller distortion (off-center displacement of the octahedral cation) in $\text{KGaF}_{1-\delta}(\text{OH})_{\delta}\text{PO}_4$ is small and the $\text{GaO}_4\text{F}_{2-\delta}(\text{OH})_{\delta}$ octahedra are essentially regular and lack the short metal-oxygen bonds characteristic of KTiOPO_4 . $\text{KGaF}_{1-\delta}(\text{OH})_{\delta}\text{PO}_4$ may be compared with the Ge^{IV} -containing KGeOPO_4 ;²⁰ in this latter phase, the GeO_6 octahedra are quite regular, with minimum and maximum Ge-O distances of 1.801(1) and 2.022(1) Å, respectively. In particular, the interoctahedral Ge-O-Ge bonds show no sign of any bond-length alternation.²⁰ An SHG of about $3 \times$ quartz was recorded² for KGeOPO_4 , and the ferroelectric \rightarrow paraelectric phase transition³³ in this phase occurs at ~ 785 °C.²⁰ Thus, the small SHG response of KGeOPO_4 is not due to the fact that this material is close to its ferroelectric Curie temperature,³⁷ above which, the SHG is identically zero in the centrosymmetric $Pnan$ paraelectric structure.³²

An interesting feature of the $\text{KGaF}_{1-\delta}(\text{OH})_{\delta}\text{PO}_4$ structure is the structural requirement for both fluoride and

hydroxide to the present in the structure, as intergallium-atom Ga-F-Ga or Ga-(OH)-Ga bridges. As was previously observed for the KTP-isostructure potassium iron fluoride phosphate, KFeFPO_4 ,³⁸ replacement of Ti^{IV} by a suitably sized trivalent cation is possible, and in this case, the interoctahedral bridging oxygen atoms are completely replaced by fluorine atoms, resulting in Fe-F-Fe bonds only and fairly regular FeO_4F_2 octahedra. For $\text{KGaF}_{1-\delta}(\text{OH})_{\delta}\text{PO}_4$, trivalent gallium may completely replace tetravalent titanium at the octahedral site. To maintain charge balance, two oxide ions must be replaced by fluoride and/or hydroxide ions, and in $\text{KGaF}_{1-\delta}(\text{OH})_{\delta}\text{PO}_4$, the two "chain" O^{2-} atoms are selectively and completely replaced by a combination of F^- and OH^- (i.e., as linking Ga-F-Ga or Ga-(OH)-Ga), which is presumably energetically favored over possible Ga-F-P or Ga-OH-P bonds. The exact details of the F/OH substitution pattern, apparently at a F:OH ratio of $\sim 0.7:0.3$ are uncertain at the microscopic level, and further work is required to determine if any preferential ordering of F and OH occur at the O/F(9) and O/F(10) sites. The new open-framework gallofluorophosphate (GaFPO) materials³⁹ offer an interesting comparison to $\text{KGaF}_{1-\delta}(\text{OH})_{\delta}\text{PO}_4$: several of these GaFPOs also contain ordered Ga-F-Ga linkages, as well as Ga-O-P bonds.

In principle, charge balance for trivalent-octahedral-cation phases crystallizing in the KTP structure would also be possible if the requisite amount of hydroxide ions replaced O^{2-} , presumably as interoctahedral M -(OH)- M links. However, the X-ray refinement described above indicates dominant fluoride ion occupation of the chain sites in $\text{KGaF}_{1-\delta}(\text{OH})_{\delta}\text{PO}_4$. Attempts to prepare $\text{KGa}(\text{OH})\text{PO}_4$ hydrothermally were unsuccessful and resulted in unknown phases, on the basis of X-ray powder measurements. Indeed, there are no KTP-type phases known of stoichiometry $M^{\text{III}}(\text{OH})\text{PO}_4$. Conversely, in the novel, partially deammoniated $(\text{NH}_4)_{1/2}\text{H}_{1/2}\text{TiOPO}_4$,⁴⁰ a Ti-(OH)-Ti link does occur, but this results from partial, completely selective loss of NH_3 from the NH_4 - TiOPO_4 structure⁴¹ and not as a requirement for charge balancing owing to trivalent-cation octahedral isomorphous substitution. This hydroxide ion has a drastic effect on the Ti(1) and Ti(2) octahedral distortions and SHG properties of $(\text{NH}_4)_{1/2}\text{H}_{1/2}\text{TiOPO}_4$.⁴⁰

On the basis of the X-ray diffraction results reported above, gallium and germanium show no preferential octahedral site-occupation effects in $\text{KGa}_{0.5}\text{Ge}_{0.5}(\text{F},\text{OH})_{0.5}\text{O}_{0.5}\text{PO}_4$, and the resulting MO_6 groups are fairly regular, without any short interoctahedral bonds. Thus, $\text{KGa}_{0.5}\text{Ge}_{0.5}(\text{F},\text{OH})_{0.5}\text{O}_{0.5}\text{PO}_4$ has a similar structure to both $\text{KGaF}_{1-\delta}(\text{OH})_{\delta}\text{PO}_4$ and KGeOPO_4 , in terms of framework geometry. The role of preferential F^- or OH^- substitution for O^{2-} is less clear in this material but is probably random over the O/F(9) and O/F(10) sites. One KTP-type phase that does show partial octahedral-cation ordering is $\text{KTi}_{0.5}\text{Sn}_{0.5}\text{PO}_4$,⁴² in which tin preferentially substitutes for titanium at one of the

(38) Matvienko, E. N.; Yakubovich, O. V.; Simonov, M. A.; Belov, N. V. *Dokl. Akad. Nauk SSSR* **1979**, *246*, 875.

(39) Loiseau, T.; Férey, G. *Eur. J. Solid State Inorg. Chem.* **1993**, *30*, 369.

(40) Eddy, M. M.; Gier, T. E.; Keder, N. L.; Stucky, G. D.; Cox, D. E.; Bierlein, J. D.; Jones, G. *Inorg. Chem.* **1988**, *27*, 1856.

(41) Harrison, W. T. A.; Phillips, M. L. F.; Gier, T. E.; Stucky, G. D.; Schultz, A. J. Unpublished work.

(37) Abrahams, S. C.; Kurtz, S. K.; Jamieson, P. B. *Phys. Rev.* **1968**, *172*, 551.

octahedral sites in a $\sim 2:1$ ratio (and vice versa at the other octahedral site).

$\text{KGa}_{0.5}\text{Ge}_{0.5}(\text{F},\text{OH})_{0.5}\text{O}_{0.5}\text{PO}_4$ is the first KTP-type material to show significant partial disorder of the guest K^+ cations over more than the two "standard" K(1) and K(2) crystallographic sites in the [001] channels. All four of the potassium cations in $\text{KGa}_{0.5}\text{Ge}_{0.5}(\text{F},\text{OH})_{0.5}\text{O}_{0.5}\text{PO}_4$ make bonds with both O/F(9) and O/F(10) (Table 5), and both K(11) and K(12) also bond to O(6), which is the only oxygen atom *not* involved in bonding to K(1), to K(2), or to both of these species, in other KTP-type phases.¹⁰ Simple bond valence arguments suggest that potassium will gain the greatest stabilization at the two eight-coordinate sites (*vide infra*). The average K–O distances for the 9-coordinate K(2) and K(11) sites are significantly longer, by about 0.1 Å, and the bond valence sums for these sites are less, by about 0.2 BVS units in each case. Thus, it would appear that the most favorable situation in $\text{KGaF}_{1-\delta}(\text{OH})_{\delta}\text{PO}_4$ would be for the K(1) and K(12) sites to be fully occupied, at the expense of the K(11) and K(2) sites, respectively. This situation is probably prevented by unfavorable $\text{K}(1)\cdots\text{K}(12)$ interactions: the two distinct K(1) to K(12) contact distances are 3.22(2) and 3.62(2) Å, the former of these being unfavorably short. By comparison, the two distinct $\text{K}(1)\cdots\text{K}(2)$ interaction distances are 3.69(1) and 3.80(1) Å, which are both physically reasonable. This K(1)/K(2) occupancy pattern is observed in the large majority of known KTP-type phases and may thus be viewed as a compromise, arising from the most favorable siting of one of the potassium cations [K(1)], while at the same time, minimizing unfavorable in-channel

$\text{K}\cdots\text{K}$ interactions [K(2) consequently preferred over K(12)].

It has been previously noted¹² that the $h(1)$ guest site is of suitable size for occupation by rubidium, and in $\text{K}_{0.84}\text{Rb}_{0.16}\text{TiOPO}_4$,³⁵ the $h(1)$ position has a small Rb occupancy. However, in $\text{KGa}_{0.5}\text{Ge}_{0.5}(\text{F},\text{OH})_{0.5}\text{O}_{0.5}\text{PO}_4$, there are no cation-size differences that might be responsible for causing K(1) and K(2) to partially disorder. This effect could be due to favorable local interactions of the potassium cation with the disordered F atoms that partially occupy the interoctahedral O/F(9) and O/F(10) sites. Alternately, it might be proposed that the K cations are partially shifting to the K(11) and K(12) to avoid *unfavorable* interactions with framework hydroxide groups [Ga/Ge–OH–Ga/Ge units], which must project into the [001] channel regions.⁴¹ The interesting $\text{K}_{0.42}\text{Na}_{0.58}\text{TiOPO}_4$, in which potassium and sodium cations occupy different, disordered channel sites, both of which are close to the "standard" K(1) and K(2) sites, depending on their different ionic radii, was described earlier.³⁰

Acknowledgment. We thank the National Science Foundation (Division of Materials Research) for partial financial support. Work at Sandia National Laboratories was supported by the US Department of Energy under Contract DE-AC04-94AL85000. We thank Hellmut Eckert (UCSB) for useful discussions and Lloyd Irwin (SNL) for carrying out the UV/visible spectroscopic measurements.

Supporting Information Available: Tables of anisotropic thermal factors for $\text{KGaF}_{1-\delta}(\text{OH})_{\delta}\text{PO}_4$ and $\text{KGa}_{0.5}\text{Ge}_{0.5}(\text{F},\text{OH})_{0.5}\text{O}_{0.5}\text{PO}_4$ (2 pages); observed and calculated structure factors (17 pages). Ordering information is given on any current masthead page.

CM950098U

(42) Crennell, S. J.; Owen, J. J.; Grey, C. P.; Cheetham, A. K.; Kaduk, J. A.; Jarman, R. H. *Eur. J. Solid State Inorg. Chem.* **1991**, *28*, 397.